A Calibration Method for Subaperture Views of Plenoptic 2.0 Camera Arrays

Sarah Fachada[1], Armand Losfeld[1], Takanori Senoh[2], Gauthier Lafruit[1] Mehrdad Teratani[1]
[1]*Laboratories of Image Synthesis and Analysis, Université Libre de Bruxelles, Brussels, Belgium*
[2]*School of Science and Technology for Future Life, Tokyo Denki University, Tokyo, Japan*

***Abstract*—We present a novel methodology to precisely calibrate the subaperture views of an array of plenoptic 2.0 cameras. Such cameras consist of a micro lens array, and the image captured through them is a lenslet image that can be converted to a dense set of pinhole views, the so-called subaperture images. This camera array provides several dense multiview images at some sparse points of 3D space. To find the relative position of those views, simply using structure-from-motion creates misalignments due to the small disparities within each set. Additionally, a traditional calibration using calibration patterns will also fail due to the complicated objectives of plenoptic 2.0 cameras and artifacts when they are converted to subaperture views. In this paper, we propose two calibration steps (a) to register the sparse central subaperture views using Structure-from-Motion which makes it robust to artifacts in the subaperture views, and (b) to register all dense multiview sets per plenoptic camera using camera's lenses specifications, disparity and distance to the scene. These two steps are followed by a novel merging process of the former registrations, to achieve precise calibration parameters for all the subaperture views of the multi-plenoptic array. Experimental results objectively and subjectively demonstrate high accuracy of the calibration. We show a 10% smaller reprojection error than using a naive structure-from-motion approach and verify that our method is suitable for high precision view synthesis applications such as virtual reality and holography.**

***Index Terms*—Plenoptic, Calibration, Light Field, Structure-from-Motion, Multiview, Virtual view, Depth Map**

I. Introduction

Plenoptic 2.0 cameras [1]–[4] allow capturing dense information within a very small distance (baseline) thanks to their micro lens array (MLA) structure. The images behind the MLA can be matched together to find precisely the 3D structure of the photographed objects. Hence, the plenoptic cameras found industrial and scientific applications, such as digital microscopy. Such cameras are also interesting in the domain of view synthesis with depth image-based rendering (DIBR) [5] as they provide, in one capture shot, several regularly spaced pinhole subaperture images. However, due to the size of the MLA, it is practically impossible to capture in one shot the occlusion information which is necessary for high quality view synthesis applications, such as virtual reality and holography, which require that the acquisitions cover a large range as in a classical camera array.

This work was partially supported by the EU project n°951989 on Interactive Technologies, H2020-ICT-2019-3, HoviTron. Sarah Fachada is a Research Fellow of the Fonds de la Recherche Scientifique - FNRS, Belgium.

To combine the advantages of classical cameras arrays with those of plenoptic cameras, a solution is hence to capture a scene with an array of plenoptic cameras. Such arrays have a potential in development of view synthesis methods using their dense capture ability with a large navigation range. Unfortunately, if the calibration between distant pinhole images is a vastly explored field [6], usual calibration methods fail to precisely register the subaperture images due to their small baseline. Camera parameters retrieval is widely explored for regular cameras. They are described with various complexity models, with and without distortion. Intrinsic camera parameters can be found using calibration patterns [7], [8] or by solving the pose-from-n-points problem [6], [9], [10].

However, to the best of our knowledge, no calibration method for subaperture views of the plenoptic 2.0 has been proposed; only a calibration method for arrays of plenoptic 1.0 [11] was recently released [12]. For plenoptic 1.0, using traditional calibration patterns is straightforward because of their simple objectives (with spatial resolution [11]). Hence, the conversion to subaperture views is as simple as pixel replacement and alignment. This approach fails with an array of plenoptic 2.0 cameras. Due to complicated objectives of such cameras (spatial-angular resolution [2]), the subaperture views converted from lenslet image will have artifacts, and consequently the detection and matching of the constraint features of the calibration pattern will not be reliable [13]. Nevertheless, it is possible to use dotted calibration patterns to calibrate the microlens array image and avoid uncertainties due to similar edges in neighbouring microlenses [13].

To make use of images captured by a plenoptic camera 2.0, several methods [4] have been designed for conversion from multilens image (aka. lenslet image captured through MLA, or sub-images) to subaperture images which is a challenging problem due to the complicated optical configuration of plenoptic 2.0 cameras [14]–[16]. As this conversion is done numerically based on adaptive block matching estimation among sub-images, it is possible to compute accurate camera parameters for the resulting multiview set, based on the camera specification, disparity and distance of the scene objects, as provided only internally in MPEG-I-Visual's work on dense light fields [17], that we release publicly in this paper.

On the other hand, to find the relative position among distant sets of subaperture views of a plenoptic 2.0 array and be robust to artifacts in the subaperture views, we propose using the Structure-from-Motion (SfM) which only relies on

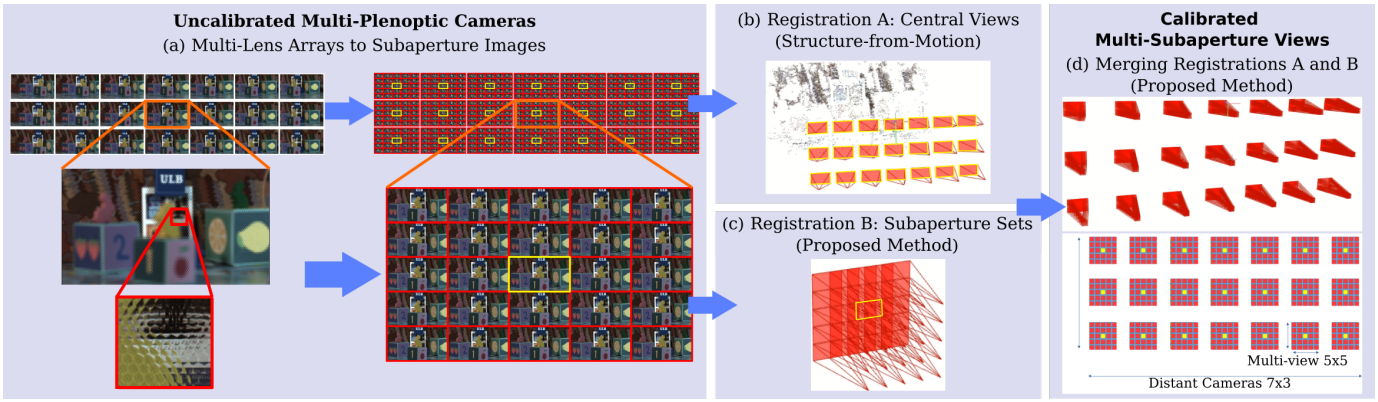

Fig. 1: Pipeline of the proposed method, from MLA to calibrated array of multiview images.

matching the natural features among images, for which complete pipelines for scene reconstruction and camera registration have been described [18], [19]. In this paper, we compute the relative pose of distant pinhole cameras using the open-source software Colmap [18], [20] - based on SfM, which shows good performances [21].

Beyond the multiview calibration for one plenoptic 2.0 camera, we present a solution to accurately compute the relative poses of the multi-plenoptic subaperture cameras, by combining two approaches that are alone insufficient to obtain the complete registration: SfM for calibration sparse central subaperture views, and calibration of all subaperture views of an individual plenoptic camera. Our method is based on matching the scene reconstructions obtained using the two approaches. Once the relative scale of each calibration is known, we merge the two models and obtain the camera parameters for the complete scene, making the dataset ready for view synthesis applications based on plenoptic 2.0 acquisition. We test our method on a natural dataset, reaching a minimum PSNR of 28dB for view synthesis applications of distant images, and 39dB for low-parallax images.

II. Proposed Calibration Method

In this section, we explain the details of our approach to calibrate the full multi-plenoptic camera dataset. The main steps of our method are shown in Fig. 1.

A. From multilens arrays to multi-subaperture views

We assume we have an array of $X \times Y$ plenoptic 2.0 cameras images. In this work, we have set $X \times Y = 7 \times 3$. The first step is the conversion from array of sub-images (lenslet image) to their corresponding subaperture multiview representation (see Fig. 1(a)). This is performed with the MPEG-I-Visual and Lenslet Video Coding software; Reference Lenslet content Convertor (RLC) [15], [16], [22]–[26]. RLC computes a set of $n \times n$ (here 5×5) subaperture views regularly spaced associated to one lenslet image. Note that the number of subaperture views will not influence the process.

B. Calibration of the central views of each subaperture set

Once the dataset is converted to a $(7 \times 3) \times (5 \times 5)$ array of pinhole views, we first register the central views of each 5×5 set (registration A, Fig. 1(b)). Those views form a 7×3 regular array of pinhole cameras. We use the software Colmap [18] to find the camera intrinsic and extrinsic parameters, assuming no distortion and centered principal point (because the images are recombined from the sub-images). We also assume that all the images of the dataset have the same intrinsic camera parameters, as they are acquired with the same camera. In order to better estimate the focal length and solve the uncertainty along the forward axis, which appears for parallel cameras [27], we added in this step seven views shot by hand-holding the camera, with random rotation and position.

Note that attempts to directly register all the subaperture views with Colmap's structure-from-motion leads to a failure and incomplete registration due to the error induced by adjacent views with small disparity. However, it is possible to first calibrate the central views of each subaperture set, then register the remaining views. We compare the reprojection error of this naive approach to the proposed one in the experiment section.

C. Calibration of the subaperture sets

In order to register the remaining images in each 5×5 sets (registration B, Fig. 1(c)), we use the method that we recently proposed internally in the context of MPEG-I-Visual standardization activities on dense light fields [17]. We describe the approach in the following. The camera parameters for the multiview images are generated from the camera specifications and the multiview image specifications, using Fig. 2, which shows the camera optical system.

For the intrinsic parameters, we use the ones found with registration A: the multiview focal length F_m (pix) and the principal point, assumed to be centered. We also define p the lenslet image pixel size (mm), $W \times H$ and $w \times h$ the multiview image size and the lenslet image size (pix). The multiview image pixel size is given by $P = p \times \frac{w}{W}$. The main lens F (mm) is given by $F = F_m \times P$. The lenslet focal length f is given by $f = F_n \times D$, where F_n is the F-number and D the diameter of the lenslet. If the lenslets have multiple F-numbers (ex. $F_n = 2.8/4/5.6$), we use the middle value. In Fig 2, s is the distance between the MLA and the image sensor and is given by $s = \frac{k \times f}{k-1}$, where k is the number of

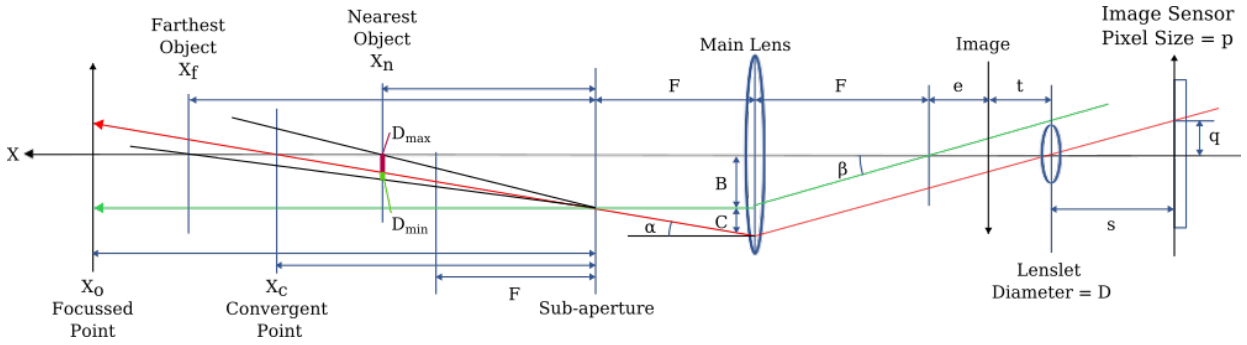

Fig. 2: Plenoptic 2.0 optical system.

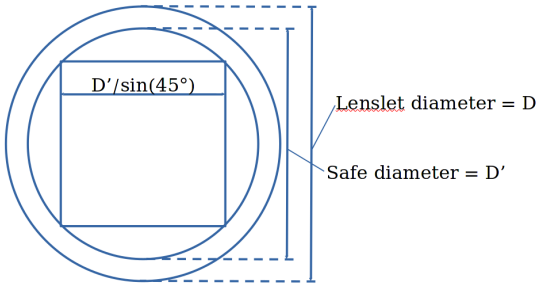

Fig. 3: Sub-image containing $N \times N$ patches of the multiview.

linearly connecting sub-images which include the same object in them. When the main lens is focusing at distance X_o from it, the image is projected at $F+e$ behind it, where $e = \frac{F^2}{X_o - F}$. The MLA further projects the image on the image sensor. The distance t between the image and the lenslet array must be $t = \frac{sf}{s-f}$ to have a sharp image on the sensor.

For the extrinsic parameters of each subaperture view, we seek the baseline B between the subaperture views and their rotation angle α as follows. As the multiview set is composed of $N \times N$ views, each lenslet image must contain all $N \times N$ viewpoints in it. Hence, the horizontal or vertical view-point distance of the lenslet center is given by $q = \frac{D' \sin(45^\circ)}{N}$ (pix), where D' is a safe diameter of lenslet (Fig. 3), because the fringe area of lenslet image is distorted in color and shape. In this experiment, D' was set to $D' = D - 2$(pix). If D', which includes the maximum disparity, is known from the lenslet-to-multiview conversion process, the result becomes more accurate.

As N is odd, we can easily trace back a ray (red in Fig. 2), passing through the lenslet center, from the first multiview point at q from the lenslet center. For simplicity, we put this lenslet center on the main lens optical axis as shown in Fig. 2. Now, the ray angle is given by $\beta = \arctan(\frac{q}{s})$. We add an additional ray (green in Fig. 2), whose angle is the same β, passing through the backside focal point F of the main lens. The main lens bends the additional (green) ray to parallel to the optical axis, and bends the first (red) ray to cross the additional ray at F in front of the main lens, where the subaperture (multiview lens) plane of this Plenoptic camera is. Now, its baseline length is given by $B = F \times \tan\beta$. The camera rotation angle is $\alpha = \arctan(\frac{C}{F})$, where $C = (e+t) \times \tan\beta$. This means that the multiview cameras are a convergent type and the convergent point distance from the subaperture plane is given by $X_c = \frac{B}{\tan\alpha}$. The multiview camera angle depends on the horizontal and vertical view position $\alpha_v = n \times \alpha$, where $n = \left[-\frac{N}{2}, +\frac{N}{2}\right]$.

The nearest/farthest object distance X_n/X_f are related to the maximum/minimum disparity $D_{\max}/D_{\min}$, which are measured by comparing the multiview images:

$$\begin{aligned} X_n &= \frac{B \times F}{C + D_{\max} \times P} \\ X_f &= \frac{B \times F}{C + D_{\min} \times P} \end{aligned} \tag{1}$$

By measuring the nearest/farthest object distance X_n/X_f and the disparity $D_{\max}/D_{\min}$, the correctness of these derived parameters can be checked by inversely solving Eq. 1:

$$B = P \frac{D_{\max} - D_{\min}}{F \times (X_n^{-1} - X_f^{-1})} \tag{2}$$

$$\alpha = \arctan\left(\frac{1}{F}\left(B \times \frac{F}{X_n} - D_{\max} \times P\right)\right) \tag{3}$$

Hence for the view j at position (h, v) in a 5×5 set of subaperture views, we get its extrinsic matrix

$$M_j^B = \begin{pmatrix} R(\alpha_h, \alpha_v) & | \, (hB, vB, 0) \\ 0, 0, 0, 1 \end{pmatrix} \tag{4}$$

where $R(\theta, \phi)$ is the rotation matrix. Note that for the central view, we obtain the identity matrix.

D. Merging the calibrations to an array of subaperture views

At this point, we have two sets of registered cameras: the 7×3 central views (registration A) and each equivalent 5×5 multiview images (registration B) (see Fig. 4(a) and (b)). Structure-from-Motion is known to perform reconstruction up to a scale, hence we cannot directly apply the transform of the central views to the 5×5 sets to get the finalized registration: we need to evaluate the scaling factor between the two registrations. To perform this precisely, we compute the depth maps for all central views of the subaperture sets using the parameters of the two registrations: using the central views in registration A, and using the surrounding subaperture

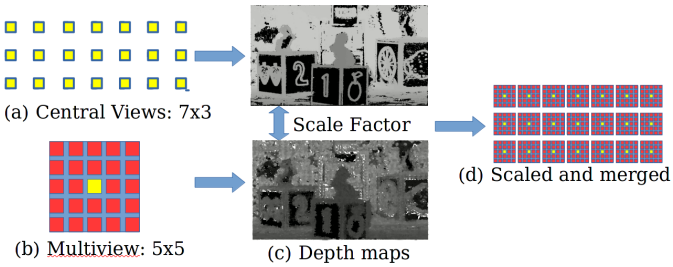

Fig. 4: Merging the two registrations. (a) The central views registration obtained with Colmap [18] (b) The multiview registration obtained with the proposed method (c) Depth maps computed with Colmap [20] for the central views in each registration (d) Merging the two models by using the scale extracted from the depth maps.

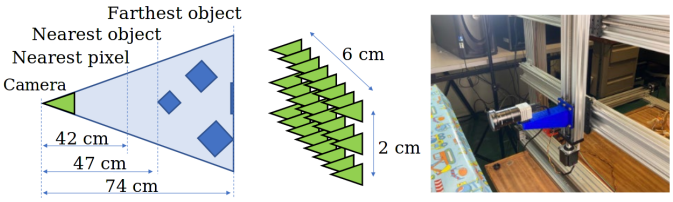

Fig. 5: Capturing condition (left) of the 7x3 multiview LL images (middle) captured by the XYZ-stage (right)

views for registration B (see Fig. 4(c)). The ratio between the two depth maps gives the scaling factor between the two registrations (see Fig. 4(d)). For a view i (center of a 5×5 subaperture set), this ratio r_i is computed on the pixels lying between the 2nd and the 9th deciles (excluding the 1st and the 10th) of each depth map (hereafter valid (img_i)) to avoid black pixels and outliers:

$$r_i = \text{Mean}_{p \in \text{valid}(\text{img}_1) \cap \text{valid}(\text{img}_2)} \left(\frac{d_2^i(p)}{d_1^i(p)} \right) \quad (5)$$

where $d_1^i(p)$ (resp. $d_2^i(p)$) is the depth of the pixel p in the view i in registration A (resp. B). Finally, we find an average ratio $r = \text{Mean}_i(r_i)$.

The final calibration is obtained by multiplying the camera position of the central views in registration A by r and applying the transformation of each central view to the registration B. Hence, for the camera i, its j^{th} view of the multiview set has the following extrinsic matrix:

$$M_{i,j} = M_i^A \times M_j^B \quad (6)$$

where M_i^A is the extrinsic of the camera i of registration A (after scaling) and M_j^B the extrinsic of camera j in registration B (identity matrix for the central views M_{13}^B).

III. Experiments

In this section, we verify the proposed method on a natural dataset. To simulate a camera array, we use a robotic XYZ-stage with a mounted plenoptic 2.0 camera, ie. Raytrix [1] (see Fig.5). We captured a lenslet image every centimeter in the vertical and horizontal directions for a total of 7×3 shots.

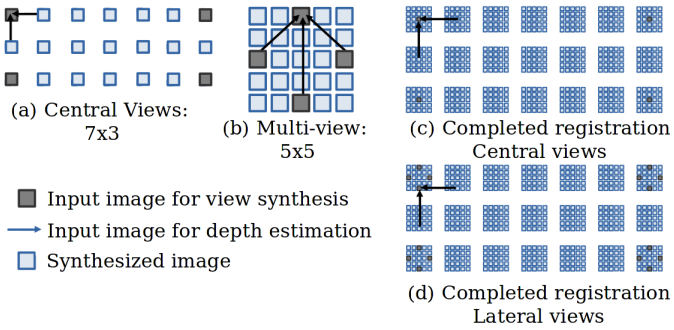

Fig. 6: Configurations used for view synthesis. (a) Validating registration A (b) Validating registration B (c) Validating overall registration with central views (d) Validating overall registration with lateral views.

Registration	A 7×3	B 5×5 **(proposed)**	Complete $(A + B)$ **(proposed)**	Complete $(A + SfM)$
Reprojection error [pix]	0.663	0.450	0.714	0.770
Number of images	$21 + 7$	25	$525 + 175$	$525 + 175$

TABLE I: Reprojection error (pix) for each calibration (intermediate registrations A and B, proposed approach and only structure-from-motion).

The scene objects were placed between 47 cm and 74 cm away from the plenoptic camera array.

After computing the camera parameters of our acquisition, we triangulated the dataset using Colmap, in order to compute the reprojection error. The error for each registration (A, B and complete) is reported in Table I. We reach lower reprojection error compared with only using Structure-from-Motion.

We verify our calibration by synthesising views of the dataset from other viewpoints, a verification strategy used in MPEG-I-Visual for the calibration the datasets meant for view synthesis applications [28], [29]. The view synthesis is done by DIBR using the Reference View Synthesis software (RVS) [30]–[32]. The depth maps are computed with the Depth Estimation Reference Software (DERS) [33]–[35]. Both software are used in MPEG-I-Visual's standardization activities for immersive video compression.

Experiment 1: To verify the registration of the central views (with Colmap [18], ie. registration A), we synthesize the central views of each multiview set from the four central views of the corners plenoptic views (see Fig. 6(a)). We

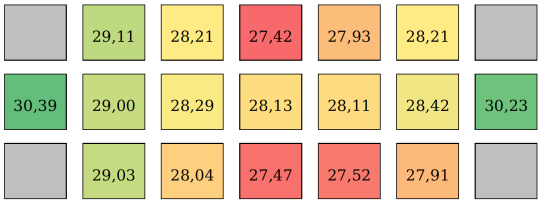

Fig. 7: Objective results (PSNR) of view synthesis using the calibration of the central views (Experiment 1).

37.47	37.71		37.39	35.30
37.37	36.88	37.57	36.71	35.22
	38.17	39.32	38.12	
37.99	37.43	38.13	37.28	35.51
35.31	35.77		36.00	34.12

Fig. 8: Objective results (PSNR) of view synthesis using the calibration per subaperture set (Experiment 2).

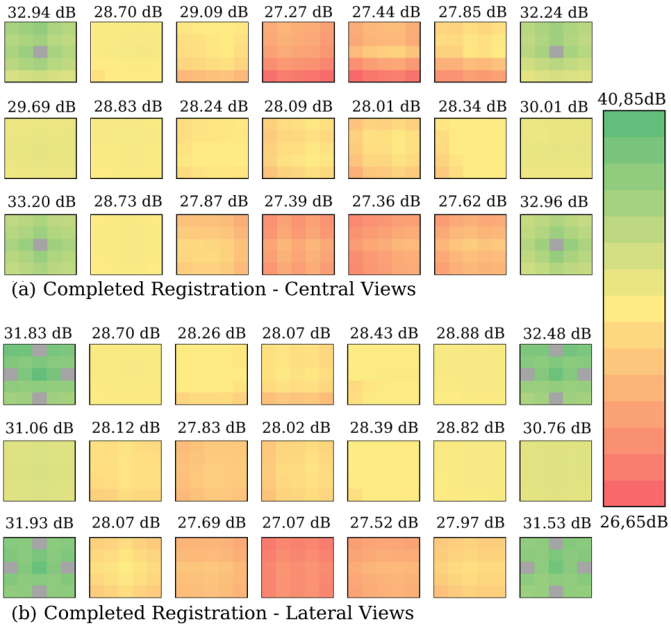

Fig. 9: Objective results (PSNR) of view synthesis using the calibration of the central views (Experiment 3).

obtain an average PSNR of 28.44dB. Details of the PSNR are given in Fig. 7. Obviously, we obtain a lower PSNR in the most distant view from the input, due to occlusions. Results verify the accuracy of the calibration among the sparse central subaperture views.

Experiment 2: To verify the proposed registration B within the multiview sets, we synthesize the views of a set from four inputs on the sides of the 5×5 square (see Fig. 6(b)). We obtain a PSNR of 36.89dB. The high values of the PSNR result from the small disparity between each view, while it verifies the accuracy of the calibration within the 5x5 views.

Experiment 3: To verify the consistency between the two registrations (A and B), we synthesize all the views of the dataset from the central viewpoints of the corners of the plenoptic array and from the lateral viewpoints of the corners of the array (see Fig. 6(c) and (d)). By this experiment, we can verify the accuracy of the proposed merging process explained in Fig. 1(d) and Fig. 4. The results are shown in Fig. 9. The view synthesis using the central viewpoints (Fig. 9(a)) takes the same input images and depth maps as the first experiment and gives similar results for the overall registration as for the

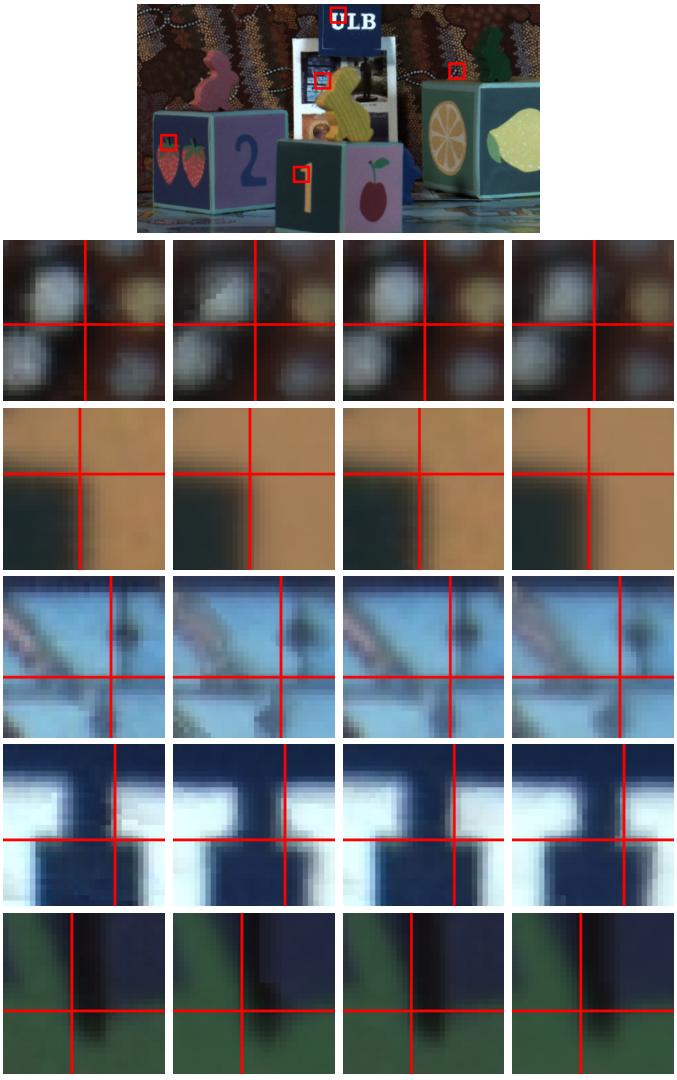

Fig. 10: Result of the view synthesis of the central view following the experiments of Fig. 6. First row: ground truth image. Following rows: zoomed details. From left to right: ground truth, calibration of the central images of each 5×5 set, calibration of the subaperture set, complete registration using the corners' lateral views.

centers calibrated with structure from motion. When using the lateral viewpoints (Fig. 9(b)), the difference in performance is imperceptible objectively (29.32dB vs. 29.98dB). Given the objective values, we can confirm the accuracy of the calibration for all subaperture views.

Finally, visual results of synthesized views are shown in Fig. 10, where the middle view of the central camera has been synthesized with RVS according to the four configurations of Fig. 6. The configurations using input images in the corners of the dataset present disocclusion artifacts due to the imperfect depth estimation on objects' borders. Zoomed details show that the precision is pixel-wise, even if the lenslet to multiview conversion induced some blur.

IV. Conclusion and future work

We have presented a novel process to calibrate the intrinsic and register the extrinsic parameters of plenoptic 2.0 camera arrays. As a result, such arrays can serve as inputs for view synthesis using dense captures with a large navigation range. In order to use such content, the proposed calibration process is designed to accurately calibrate and register multiple sets of dense multiview images, converted from multi-plenoptic cameras' views. We proposed a merging process that combines the classical structure-from-motion for calibration of the distant cameras, and another calibration approach that we proposed for the subaperture images of one plenoptic camera. Experimental results verify the accuracy of the process, objectively and subjectively.

In order to further improve the accuracy of the calibration, we will consider a more complete camera model to address distortion caused by the main lens and the micro lens array. We plan to release the complete tool to MPEG and make it publicly available in our repository.

References

[1] Raytrix, *Raytrix*, 2019. [Online]. Available: https://raytrix.de/

[2] A. Lumsdaine and T. Georgiev, "The focused plenoptic camera," in *2009 IEEE International Conference on Computational Photography (ICCP)*. San Francisco, CA, USA: IEEE, Apr. 2009, pp. 1–8. [Online]. Available: http://ieeexplore.ieee.org/document/5559008/

[3] C. Perwass and L. Wietzke, "Single lens 3d-camera with extended depth-of-field," in *Human Vision and Electronic Imaging XVII*, vol. 8291. International Society for Optics and Photonics, 2012, p. 829108.

[4] C. Conti, L. D. Soares, and P. Nunes, "Dense Light Field Coding: A Survey," *IEEE Access*, vol. 8, pp. 49 244–49 284, 2020.

[5] C. Fehn, "Depth-image-based rendering (DIBR), compression, and transmission for a new approach on 3D-TV," in *Stereoscopic Displays and Virtual Reality Systems XI*, vol. 5291. International Society for Optics and Photonics, May 2004, pp. 93–105.

[6] R. Hartley and A. Zisserman, "Multiple view geometry in computer vision," *Cambridge Univ.Press*, 2000.

[7] J. Weng, P. Cohen, M. Herniou *et al.*, "Camera calibration with distortion models and accuracy evaluation," *IEEE Transactions on pattern analysis and machine intelligence*, vol. 14, no. 10, pp. 965–980, 1992.

[8] Z. Zhang, "A flexible new technique for camera calibration," *IEEE Transactions on pattern analysis and machine intelligence*, vol. 22, no. 11, pp. 1330–1334, 2000.

[9] H. C. Longuet-Higgins, "A computer algorithm for reconstructing a scene from two projections," *Nature*, vol. 293, no. 5828, pp. 133–135, 1981.

[10] O. Ozyesil, V. Voroninski, R. Basri, and A. Singer, "A survey of structure from motion," *arXiv preprint arXiv:1701.08493*, 2017.

[11] R. Ng, M. Levoy, M. Brédif, G. Duval, M. Horowitz, and P. Hanrahan, "Light field photography with a hand-held plenoptic camera," Ph.D. dissertation, Stanford University Computer Science Tech Report CSTR, feb 2005.

[12] W. Darwish, Q. Bolsee, and A. Munteanu, "Plenoptic Camera Calibration Based on Sub-Aperture Images," in *2019 IEEE International Conference on Image Processing (ICIP)*. Taipei, Taiwan: IEEE, Sep. 2019, pp. 3527–3531. [Online]. Available: https://ieeexplore.ieee.org/document/8803473/

[13] C. Heinze, S. Spyropoulos, S. Hussmann, and C. Perwaß, "Automated Robust Metric Calibration Algorithm for 3D Camera Sytems," *IEEE Transactions on Instrumentation and Measurement*, vol. 65, no. 5, pp. 1197–1205, 2016.

[14] L. Palmieri, R. Koch, and R. O. H. Veld, "The plenoptic 2.0 toolbox: Benchmarking of depth estimation methods for mla-based focused plenoptic cameras," in *2018 25th IEEE International Conference on Image Processing (ICIP)*. IEEE, 2018, pp. 649–653.

[15] M. Teratani, S. Fujita, W. Ouyang, K. Takahashi, and T. Fujii, "3D Imaging System using Multi-focus Plenoptic Camera and Tensor Display," in *2018 International Conference on 3D Immersion (IC3D)*, Dec. 2018, pp. 1–7, iSSN: 2379-1780.

[16] M. Teratani and T. Fujii, "[MPEG-I Visual] Conversion of Lenslet Data Capture by Single-Focused Plenoptic Camera to Multiview video Using RLC0.3 [N18567]," *ISO/IEC JTC1/SC29/WG11*, Jul. 2019.

[17] T. Senoh and N. Tetsutani, "[DLF] Camera Parameter Generation from Plenoptic2 Image [M56349]," *ISO/IEC JTC1/SC29/WG11*, p. 15, Apr. 2021.

[18] J. L. Schönberger and J.-M. Frahm, "Structure-from-motion revisited," in *Conference on Computer Vision and Pattern Recognition (CVPR)*, 2016.

[19] *Capturing Reality*. [Online]. Available: http://www.capturingreality.com

[20] J. L. Schönberger, E. Zheng, M. Pollefeys, and J.-M. Frahm, "Pixelwise view selection for unstructured multi-view stereo," in *European Conference on Computer Vision (ECCV)*, 2016.

[21] E.-K. Stathopoulou, M. Welponer, and F. Remondino, "Open-Source Image-Based 3D Reconstruction Pipelines: Review, Comparison and Evaluation," *ISPRS - International Archives of the Photogrammetry, Remote Sensing and Spatial Information Sciences*, vol. XLII-2/W17, pp. 331–338, Nov. 2019. [Online]. Available: https://www.int-arch-photogramm-remote-sens-spatial-inf-sci.net/XLII-2-W17/331/2019/

[22] M. Teratani, W. Ouyang, and T. Fujii, "[MPEG-I Visual] Manual of Reference Lenslet Content Convertor (RLC0.3)," *ISO/IEC JTC1/SC29/WG11*, Oct. 2019.

[23] S. Fachada, D. Bonatto, G. Lafruit, and M. Teratani, "[DLF] Update for Reference Lenslet content Convertor (RLC) [M56418]," *ISO/IEC JTC1/SC29/WG11*, Apr. 2021.

[24] *RLC 0.3*. [Online]. Available: https://www.fujii.nuee.nagoya-u.ac.jp/multiview-data/Raytrix/RLC0.3.zip

[25] *RLC 1.0*. [Online]. Available: https://gitlab.com/mpeg-dense-light-field/rlc

[26] S. Fujita, S. Mikawa, M. Panahpourtehrani, K. Takahashi, and T. Fujii, "Extracting multi-view images from multi-focused plenoptic camera," in *International Forum on Medical Imaging in Asia 2019*, vol. 11050. International Society for Optics and Photonics, 2019, p. 1105006.

[27] F. Dai and M. Lu, "Photo-based 3d modeling of construction resources for visualization of operations simulation: Case of modeling a precast façade," in *2008 Winter Simulation Conference*. IEEE, 2008, pp. 2439–2446.

[28] D. Doyen, G. Boisson, and G. Gendrot, "New version of the pseudo-rectified TechnicolorPainter content [M43366]," *ISO/IEC JTC1/SC29/WG11*, Jul. 2018.

[29] A. Schenkel, S. Fachada, and G. Lafruit, "ULB Unicorn v2 updated camera parameters [M42310]," *ISO/IEC JTC1/SC29/WG11*, p. 14, Apr. 2018.

[30] S. Fachada, D. Bonatto, A. Schenkel, and G. Lafruit, "Depth Image Based View Synthesis With Multiple Reference Views For Virtual Reality," in *2018-3DTV-Conference: The True Vision-Capture, Transmission and Display of 3D Video (3DTV-CON)*. Stockholm, Sweden: IEEE, 2018.

[31] B. Kroon, "Reference View Synthesizer (RVS) manual [N18068]," *ISO/IEC JTC1/SC29/WG11*, p. 19, Oct. 2018.

[32] D. Bonatto, S. Fachada, and G. Lafruit, "RaViS: Real-time accelerated View Synthesizer for immersive video 6DoF VR," *Electronic Imaging*, vol. 2020, no. 13, pp. 382–1–382–9, 2020. [Online]. Available: https://www.ingentaconnect.com/content/ist/ei/2020/00002020/00000013/art00012

[33] T. Senoh, K. Yamamoto, N. Tetsutani, and H. Yasuda, "Enhanced DERS for quad reference views (eDERS)," *ISO/IEC JTC1/SC29/WG11*, Jan. 2018.

[34] S. Rogge, D. Bonatto, J. Sancho, R. Salvador, E. Juarez, A. Munteanu, and G. Lafruit, "MPEG-I Depth Estimation Reference Software," in *2019 International Conference on 3D Immersion (IC3D)*. Brussels, Belgium: IEEE, Dec. 2019, pp. 1–6. [Online]. Available: https://ieeexplore.ieee.org/document/8975995/

[35] E. Juarez, "Manual of Depth Estimation Reference Software (DERS 8.0) [N18450]," *ISO/IEC JTC1/SC29/WG11*, Mar. 2019.